View metadata, citation and similar papers at core.ac.uk

brought to you by CORE

provided by Elsevier - Publisher Connector

FEBS Letters 587 (2013) 3142–3147

FEBS Letters

journal homepage: www.FEBSLetters.org

Nicotinamide is a specific inhibitor of dark-operative protochlorophyllide oxidoreductase, a nitrogenase-like enzyme, from *Rhodobacter capsulatus*

Jiro Nomata [a,1], Toru Kondo [b,2], Shigeru Itoh [b,3], Yuichi Fujita [a,*]

[a] *Graduate School of Bioagricultural Sciences, Nagoya University, Nagoya 464-8601, Japan*
[b] *Graduate School of Science, Nagoya University, Nagoya 464-8602, Japan*

ARTICLE INFO

Article history:
Received 6 June 2013
Revised 30 July 2013
Accepted 31 July 2013
Available online 14 August 2013

Edited by Richard Cogdell

Keywords:
Bacteriochlorophyll
Chlorophyll
FeS cluster
Nitrogenase
Protochlorophyllide

ABSTRACT

Dark-operative protochlorophyllide oxidoreductase (DPOR) is a nitrogenase-like enzyme consisting of two components, L-protein as a reductase component and NB-protein as a catalytic component. Elucidation of the crystal structures of NB-protein (Muraki et al., Nature 2010, 465: 110–114) has enabled us to study its reaction mechanism in combination with biochemical analysis. Here we demonstrate that nicotinamide (NA) inhibits DPOR activity by blocking the electron transfer from L-protein to NB-protein. A reaction scheme of DPOR, in which the binding of protochlorophyllide (Pchlide) to the NB-protein precedes the electron transfer from the L-protein, is proposed based on the NA effects.
© 2013 Federation of European Biochemical Societies. Published by Elsevier B.V. All rights reserved.

1. Introduction

Chlorophylls (Chls) and bacteriochlorophylls (Bchls) are tetrapyrrole pigments essential for photosynthesis [1,2]. Nitrogenase-like three-subunit enzymes play a critical role in the formation of parental structures, which are of chlorin and bacteriochlorin, in their biosynthetic pathways of Chl and Bchl, respectively [3,4]. Dark-operative protochlorophyllide oxidoreductase (DPOR) converts porphyrin to chlorin by the stereo-specific reduction of C17=C18 double bond of Pchlide to form chlorophyllide *a* (Chlide) (Fig. 1A) [5,6]. Since the spectroscopic property of Chl *a* is identical to that of Chlide, DPOR is regarded as the enzyme catalyzing the final step to form the spectroscopic property of Chl *a* in Chl *a* biosynthesis. Oxygenic photosynthetic organisms harbor an alternative Pchlide reductase called the light-dependent Pchlide oxidoreductase (LPOR), a single polypeptide enzyme belonging to the short-chain dehydrogenase/reductase family [7,8]. Since the structures and the probable reaction mechanisms of LPOR and DPOR are completely different, it has been suggested that photosynthetic organisms evolved independently the two distinct Pchlide reductases [9]. In Bchl *a* biosynthesis in anoxygenic photosynthetic bacteria, the chlorin, Chlide, is further converted to bacteriochlorin, 3-vinyl bacteriochlorophyllide *a*, by the reduction of C7=C8 double bond, which is catalyzed by another nitrogenase-like enzyme Chlide oxidoreductase [10,11].

DPOR consists of two separable components, one is an ATP-dependent reductase component called L-protein (ca 70 kDa; a BchL dimer) and the other is a catalytic component called NB-protein (ca 230 kDa; a BchN-BchB heterotetramer). L-protein and NB-protein represent structural cognates of Fe protein and MoFe protein of nitrogenase, respectively [12,13]. L-protein and NB-protein of DPOR resemble Fe protein and MoFe protein of nitrogenase, respectively, in crystal structure [5,6,14]. The structural features of DPOR suggested the electron transfer pathway from the [4Fe–4S] cluster of L-protein to Pchlide via the NB-cluster, which is similar

Abbreviations: Bchl, bacteriochlorophyll; Chl, chlorophyll; Chlide, chlorophyllide *a*; DPOR, dark-operative protochlorophyllide oxidoreductase; LPOR, light-dependent protochlorophyllide oxidoreductase; NA, nicotinamide; Pchlide, protochlorophyllide

* Corresponding author. Fax: +81 52 789 4107.
E-mail address: fujita@agr.nagoya-u.ac.jp (Y. Fujita).
[1] Present address: Chemical Resources Laboratory, Tokyo Institute of Technology, Yokohama 226-8503, Japan.
[2] Present address: Department of Physics, Tokyo Institute of Technology, O-okayama, Meguro-ku, Tokyo 152-8550, Japan.
[3] Present address: Center for Gene Research, Nagoya University, Nagoya 464-8602, Japan.

0014-5793/$36.00 © 2013 Federation of European Biochemical Societies. Published by Elsevier B.V. All rights reserved.
http://dx.doi.org/10.1016/j.febslet.2013.07.054

to that from the [4Fe–4S] cluster of Fe protein to FeMo-co via the P-cluster in nitrogenase [5]. The crystal structure of a ADP–AlF_3-stabilized complex of L-protein and NB-protein supports the hypothesis [15]. The [4Fe–4S] cluster of the L-protein is reduced by ferredoxin *in vivo* or dithionite *in vitro* [12,13], and the electron is transferred to the NB-cluster in the NB-protein through a transient complex formation between the L-protein and the NB-protein. This inter-subunit electron transfer is coupled with ATP hydrolysis by the L-protein. The substrate Pchlide is accommodated in the binding cavity that is located about 10 Å distant from the NB-cluster in the NB-protein [5]. The binding cavity is surrounded by many hydrophobic residues. Upon the binding of Pchlide, an a helix of BchB′ is partly unwound to allow the interaction of some residues of Met408-Leu410 in the helix with the Pchlide molecule. Some residues (BchN-Trp387 and BchN-Phe393) protruding into the cavity also undergo a noticeable conformational change induced by the binding of Pchlide [5].

The stereospecificity of the C17=C18 double bond reduction is determined by the spatial arrangement of the proton donors. According to the hypothesis, BchB′-Asp274 and the C17-propionate of the substrate Pchlide itself donate protons to C17 and C18, respectively, to form the *trans*-reduced Chlide. However, it remains unknown how the transfer events of two protons and two electrons are coordinated to complete the double bond reduction. For the detailed study of reaction mechanism of DPOR, specific inhibitors of the reaction would be effective, while only Chl *c* has been known as a specific inhibitor of DPOR [5].

The early studies on Bchl biosynthesis using photosynthetic bacteria suggested that the cells of *Rhodobacter sphaeroides* [16] and *Rubrivivax gelatinosus* (*Rhodopseudomonas gelatinosa*) [17] grown in the presence of nicotinamide (NA) excreted divinyl Pchlide (8-vinyl Pchlide) to the outer media. These phenomena are now thought to occur by the inhibition of the Pchlide reduction by NA, but there has been no experimental evidence supporting this possibility so far.

We determined that NA inhibits the DPOR reaction by blocking the electron transfer from L-protein to NB-protein based on the kinetics and EPR analyses. The results suggest that the binding of Pchlide to NB-protein precedes the docking of the L-protein to the NB-protein for the electron transfer. In addition, we predicted the NA binding site on the NB-protein based on the results and the crystal structures.

2. Materials and methods

2.1. Bacterial strains and culture conditions

A photosynthetic competent mutant DB176 of *Rhodobacter capsulatus* [18,19] and *E. coli* JM105 [20] were used to overexpress L-protein and NB-protein.

2.2. Purification of L-protein and NB-protein

Crude extracts were prepared and the L-protein and the NB-protein were purified as described previously [18–20]. Protein concentrations were determined using the BCA method (Protein Assay; Bio-Rad), with bovine serum albumin as the standard. Protein purity was monitored by SDS–PAGE (Fig. 1B, inset).

2.3. DPOR assay with NA

Assays of DPOR activity were carried out essentially as described previously [18–20], except that the reaction medium contained 0–500 μM NA, 2.9–40 μM Pchlide. DPOR assays were carried out at 34 °C for 9 or 6 min, and the amount of formed Chlide was estimated from the absorption spectra of hexane-extracted acetone phase [13].

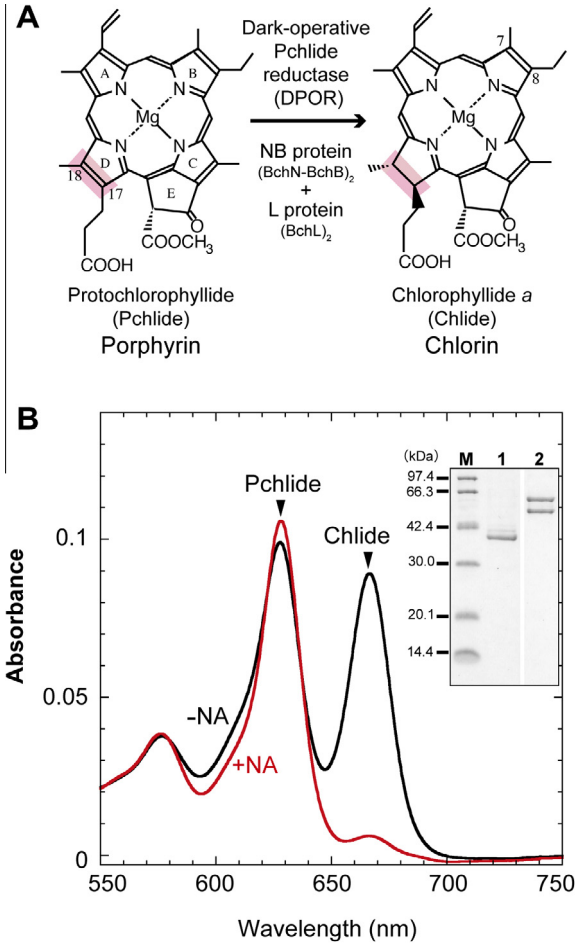

Fig. 1. (A) The reaction of Pchlide reduction. The C17=C18 double bond of Pchlide is stereospecifically reduced by DPOR to form Chlide, the direct precursor of Chl *a* in oxygenic photosynthetic organisms. In Bchl *a* biosynthesis Chlide is further reduced to 3-vinyl bacteriochlorophyllide *a* by Chlide oxidoreductase, another nitrogenase-like enzyme. (B) Inhibition of DPOR activity by NA. DPOR assay was carried out with purified L-protein and NB-protein in the absence (black line) or presence (500 μM, red line) of NA. The reactions were stopped by the addition of acetone and the absorption spectra were recorded. Inset. SDS–PAGE profile of the affinity purified L-protein (lane 1; 1 μg) and NB-protein (lane 2; 2.5 μg).

2.4. EPR spectroscopy

EPR samples were prepared as described previously [21]. The reaction mixtures were incubated for 10 min at 5 °C and frozen rapidly in liquid nitrogen to quench the reaction, and EPR spectra were recorded using a Bruker ESP-300E X-band spectrometer (Bruker Biospin, Germany) with a 100 kHz field modulation equipped with a liquid-helium flow cryostat (CF935, Oxford Instruments, Oxford, UK).

3. Results

Using the assay system with the purified L-protein and NB-protein described previously [18–20], we examined the effect of NA for the Pchlide reduction. DPOR activity was significantly reduced in the presence of NA (500 μM) (Fig. 1B). Dependency of DPOR activity on Pchlide concentration was measured in the presence of four different concentrations of NA to determine the inhibition mechanism. Apparent K_m and V_{max} values were decreased with increasing NA concentration. The double-reciprocal plot gave the multiple parallel lines (Fig. 2A), indicating that NA is an uncompetitive inhibitor to Pchlide. This uncompetitive inhibition suggested

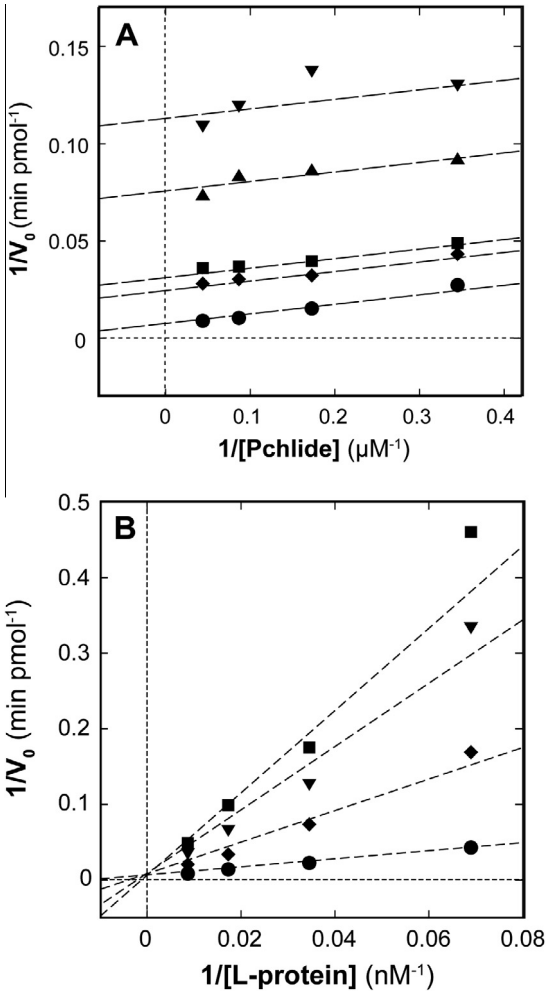

Fig. 2. (A) Lineweaver–Burk plot with the parallel lines shows the characteristic uncompetitive inhibition of DPOR reaction by NA. L-protein (6.7 μg) and NB-protein (9.1 μg) were prepared from *R. capsulatus* DB178. Final concentrations of L-protein and NB-protein in the reactions were 400 and 170 nM, respectively. The concentrations of NA were maintained constant in a subset of lines (●, 0 μM; ♦, 67 μM; ■, 100 μM; ▲, 300 μM; and ▼, 500 μM), while the concentrations of Pchlide were varied. K_m for Pchlide, V_{max} and K_i were estimated to be 12.1 μM, 20 nmol min^{-1} mg$_{NB\text{-}protein}^{-1}$ and 37 μM, respectively. (B) Lineweaver–Burk plot illustrating the intersecting lines shows the characteristic competitive inhibition of DPOR by NA. L-protein and NB-protein were prepared from *E. coli*. In this assay, concentration of L-protein, which was regarded as the substrate, was varied at the fixed concentration of NB-protein (29 nM). The concentration of NA was maintained in a subset of lines (●, 0 μM; ♦, 50 μM; ▼, 100 μM; and ■, 150 μM), while the concentration of L-protein was varied (15–118 nM). K_m for L-protein, V_{max} and K_i were estimated to be 92 nM, 119 nmol min^{-1} mg$_{NB\text{-}protein}^{-1}$ and 10 μM, respectively.

that NA inhibits the DPOR activity by the binding to the Pchlide-bound NB-protein rather than to the Pchlide-free NB-protein.

To study the inhibition mechanism by NA, we measured DPOR activity at various L-protein concentrations in the presence and absence of NA. In this reaction, L-protein can be regarded as the substrate for the enzyme NB-protein. Apparent V_{max} values were constant while apparent K_m values were increased with the increase of concentration of NA. The double reciprocal plot showed multiple lines with a common intercept on the $1/V_0$ axis with different slopes (Fig. 2B), indicating that NA is a competitive inhibitor to L-protein. This suggested that NA binds to the Pchlide-bound NB-protein competing with L-protein. As a consequence, NA binding to the NB-protein would block the electron transfer from L-protein to NB-protein and inhibits the Pchlide reduction.

Electron paramagnetic resonance (EPR) spectroscopy was performed in the presence and absence of NA to directly measure

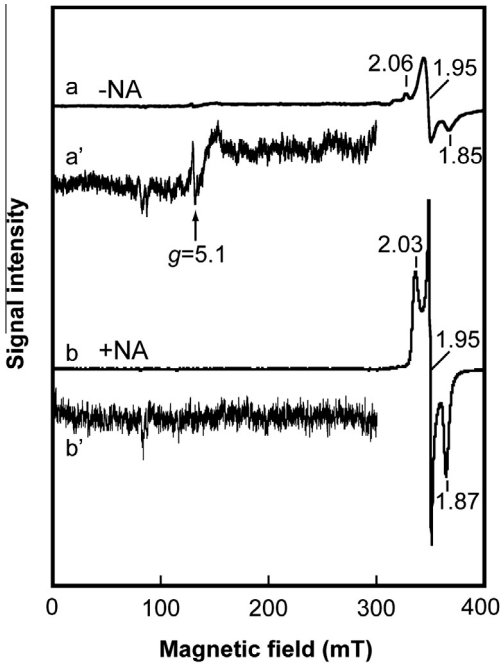

Fig. 3. EPR spectra of the DPOR assay in the presence (traces b and b′) or absence (traces a and a′) of NA. EPR spectra were measured in the DPOR assay mixture containing NB-protein (7.9–10 μM), L-protein (20–22 μM), Chl *c* (10–20 μM) and NA (28 mM). The spectra (traces a and b) are 26.7 times enlarged (traces a′ and b′) to show the $g = 5.1$ signal clearly. Experimental condition for the measurement: microwave power, 20 mW; microwave frequency, 9.510 GHz (trace a) and 9.562 GHz (trace b); modulation amplitude, 2 mT at 100 kHz; time constant, 20 ms. The traces a and b represent the average of 10 and 3 scans, respectively.

the effect of NA on the electron transfer from L-protein to NB-protein. NB-protein has a unique [4Fe–4S] cluster called NB-cluster that is held by three Cys from BchN and one Asp from BchB. NB-cluster shows a broad $S = 3/2$ signal and a narrow signal of $g = 5.1$ only in the reaction mixture containing Chl *c*, which act as a competitive inhibitor with the substrate Pchlide [21]. In the absence of NA the narrow signal of $g = 5.1$, which is specific for the NB-cluster, was clearly detected. The broad signal was not evident under this condition due to the lower concentration of NB-protein than used in the previous study (Fig. 3, trace a′). In addition, an $S = 1/2$ signal was also detected at $g = 2.06$, 1.95 and 1.85. On the other hand, in the presence of NA, the NB-protein did not show the narrow signal of $g = 5.1$ (Fig. 3, trace b′), and the $S = 1/2$ signal ($g = 2.03$, 1.95 and 1.87) was markedly increased (Fig. 3, trace b). The shape and *g*-values of the $S = 1/2$ signal were almost similar to those reported for the reduced [4Fe–4S] cluster of the L-protein [18]. Thus, the result indicates that the ratio of the reduced form to the oxidized form of the [4Fe–4S] cluster of L-protein was much higher in the NA+ sample than that in the NA− sample. The loss of the NB-cluster signal and the increase of the [4Fe–4S] cluster signal of L-protein suggest that the electron transfer from the [4Fe–4S] cluster in L-protein to the NB-cluster of NB-protein is blocked by NA (Fig. 4A). These results support the inhibition mechanism suggested by the kinetic experiments (Fig. 2).

4. Discussion

NA inhibits DPOR activity by blocking of the electron transfer from L-protein to NB-protein in this report. In some purple bacteria, the addition of NA induced Pchlide accumulation and decreased Bchl [16,17]. The preferential accumulation of a divinyl form of Pchlide than its monovinyl form lead to the conclusion that NA inhibits the divinyl reductase that converts divinyl Pchlide to

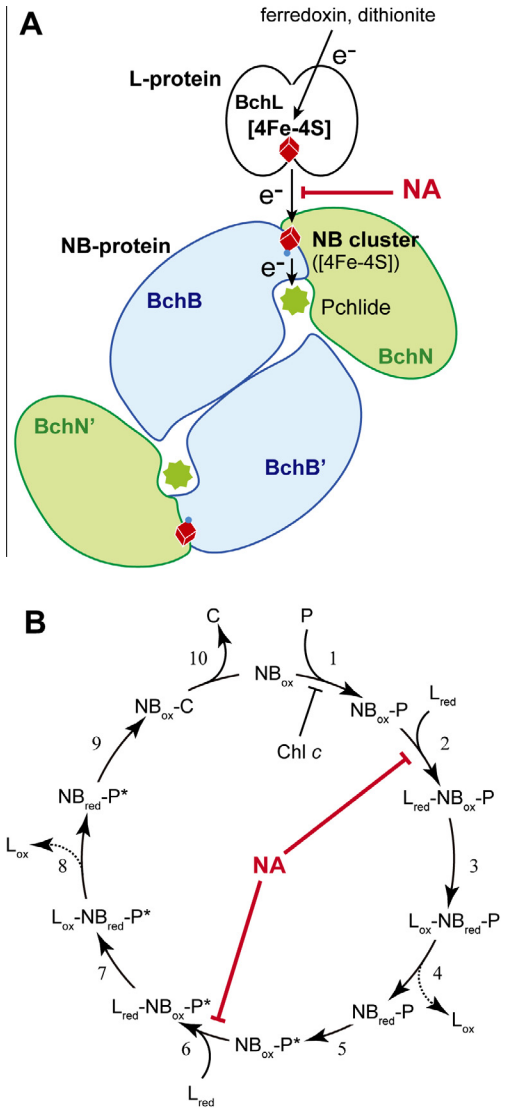

Fig. 4. Reaction scheme of the DPOR cycle. (A) Schematic model of DPOR. The [4Fe–4S] clusters are shown by red cubes. The blue dots of the NB-cluster represent the unique Asp coordination. Pchlide is shown by pale green octagons. NB-protein is shown as a symmetrical dimer complex of two functional units as BchN-BchB and BchN′-BchB′. The electron transfer scheme is shown for only one functional unit. (B) In this scheme, we focus only on the bound and redox states of L-protein and NB-protein by neglecting other details such as ATP hydrolysis and proton transfer events of Pchlide. L, NB, P and C indicate L-protein, NB-protein, Pchlide and Chlide, respectively. Probable redox states of L-protein and NB-protein are shown by subscripts, ox and red. Dissociation of L-protein from NB-protein could occur at step 4 or 5 in the 1st cycle and at step 8 or 9 in the 2nd cycle, which are shown tentatively by dotted lines in steps 4 and 8, respectively. Some intermediate states of Pchlide, which is generated after the first electron transfer step, are shown as P*, including both radical and protonated states of Pchlide. NA blocks the binding steps of L-protein to NB-protein, steps 2 and 6, while Chl *c* blocks step 1 by competitive inhibition.

monovinyl Pchlide, in addition to the inhibition of the reduction C17=C18 double bond of Pchlide. However, our *in vitro* assay with the purified components in this study clearly demonstrated that NA inhibits the DPOR activity (Fig. 1B).

DPOR has a structure resembling that of nitrogenase. DPOR catalyzes a simple two-electron reduction while nitrogenase catalyzes the eight-electron reduction. Therefore, the reaction mechanism of DPOR will be a guide for understanding the complex reaction mechanism of nitrogenase as well as another simple nitrogenase-like enzyme the NifEN complex [22].

Specific inhibitors have been useful tools to investigate the reaction mechanism of enzymes. In the case of nitrogenase, Fe protein and MoFe protein do not form a stable complex during the catalytic cycle, and the ATP-dependent electron transfer occurs through a transient complex formation between the components. ATP analogues such as ADP aluminium fluoride (ADP–AlF_4) inhibit the nitrogenase reaction by stabilizing the complex between Fe protein and MoFe protein. The crystal structures of the Fe-protein and MoFe protein complex stabilized by ADP–AlF_4 have revealed the specific recognition mechanism coupled with ATP hydrolysis that ensures the electron transfer from Fe protein to MoFe protein [23–25]. Similarly, L-protein and NB-protein of DPOR also do not form a stable enzyme complex during the catalytic cycle [13]. This is supported by the observation that the NB-protein requires the L-protein more than 3 in a molar ratio for the maximal activity [19]. The complex between the L-protein and the NB-protein, which is a hexameric complex of $[(ChlL)_2(ChlN\text{-}ChlB)]_2$ from *Prochlorococcus marinus*, is stabilized by the addition of ADP-AlF_3 similar to nitrogenase, which allowed crystallographic analysis [15]. This complex structure brought new insight into the complex formation mechanism of the DPOR components.

A Pchlide analogue, Chl *c*, also inhibits the DPOR reaction. Chl *c* binds to a substrate pocket of NB-protein in a competition with Pchlide and inhibits the Pchlide reduction. The inhibitory action of Chl *c* has provided compelling evidence for the role of the C17-propionate as the proton donor for C18 [5]. The unique EPR signal from the NB-cluster, which acts as an electron mediator from the L-protein to Pchlide, can be detected in the presence of Chl *c* [21].

The kinetic analysis together with EPR spectroscopy suggested that NA has no effect on the Pchlide binding while interfering with the electron transfer from the [4Fe–4S] cluster of L-protein to the NB-cluster. Indeed, the absorption spectrum of the Pchlide-bound NB-protein remained unchanged upon the addition of NA (data not shown), which is consistent with the idea that NA is not involved in the Pchlide binding. Thus, NA provides a promising system to investigate the intra-molecular electron transfer mechanism in the NB-protein by blocking the electron flow from L-protein.

We formulated a scheme for the DPOR reaction (Fig. 4B) based on the inhibitory effect of NA revealed in the present study. As the first step (step 1), the substrate Pchlide is bound to the Pchlide-free form of NB-protein (an oxidized form), prior to the binding of L-protein. This binding of Pchlide in the substrate cavity on the NB-protein may trigger some conformational changes to increase the affinity of a L-protein docking site on the surface of NB-protein. The second (step 2) is the binding of L-protein (a reduced form) to the L-protein docking site on the NB-protein to form a ternary complex, L-protein-NB-protein-Pchlide. In step 3, the electron is transferred from L-protein to NB-protein (the NB-cluster). In step 4, the oxidized L-protein is dissociated from the NB-protein. This dissociation process could occur in step 5. Then, the oxidized L-protein is re-reduced by dithionite and re-binds to the NB-protein to transfer the second single electron to the NB-protein (steps 6–8). These two reactions of the L-protein, which achieve the two successive one-electron reduction of the NB-protein, cooperate to convert Pchlide to Chlide (step 9). Finally, Chlide is released from the oxidized NB-protein (step 10). Two proton transfer events should also be coupled to the electron transfer events (steps 5 and 9). NA competitively inhibits the binding of L-protein to the docking site of the NB-protein (steps 2 and 6), and blocks the electron transfer from the L-protein to the NB-protein. The scheme interprets the DPOR reaction well.

Based on this kinetic study we try to predict the NA binding site on the NB-protein. The results in this study provided two clues: (1) NA binds to the Pchlide-bound NB-protein more tightly than to the

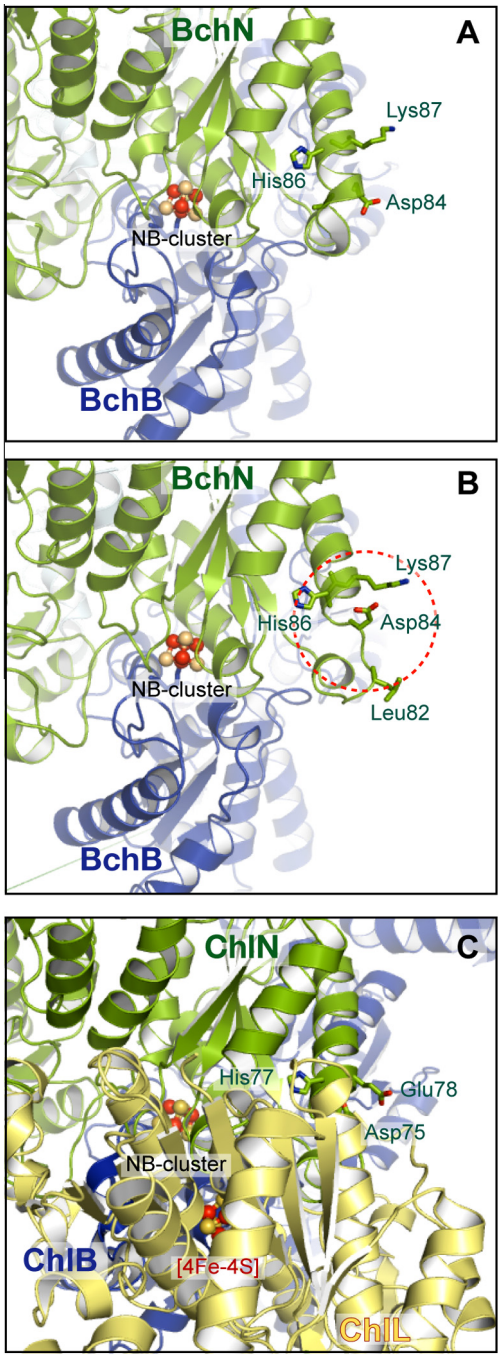

Fig. 5. Probable NA binding site on the NB-protein from *R. capsulatus*. (A) The Pchlide-free form (4AER). (B) The Pchlide-bound form (4AEK). The three amino acid residues of BchN, Asp84, His86 and Lys87, are shown. Proposed NA binding site is shown by the dashed red circle. (C) The corresponding region of the L-protein–NB-protein complex from *P. marinus* (2YNM) [15]. The three amino acid residues, Asp75, His77 and Glu78, corresponding to Asp84, His86 and Lys87 in ChlN are shown. These residues are involved in the interaction with the L-protein. The [4Fe–4S] cluster in the L-protein is also shown.

Pchlide-free NB-protein, which suggests that the NA binding site in the NB-proteins undergoes some conformational changes upon Pchlide binding, and (2) NA competes with the L-protein in binding to the Pchlide-bound NB-protein. We can consider two additional possibilities: (3) The NA binding site may be located in the L-protein docking region on the NB-protein, and (4) NA may bind to the NB-protein in a similar manner as in other NA-binding proteins whose crystal structures are available. In most of these NA-binding proteins, NA is mainly stabilized by two hydrogen bonds between its amino group and either of Asp/Glu residues and between its oxo group and either of Arg/Lys/His residues [26]. Therefore, we propose the NA binding site to be in the vicinity of a triad of BchN-Asp84, BchN-His86 and BchN-Lys87 (Fig. 5AB). Significant conformational differences were found in a loop (Ala80 to Ala85) containing Asp84 of BchN between the Pchlide-bound and Pchlide-free NB-proteins. The distances between Asp84 and His86, and between Asp84 and Lys87 become significantly shorter upon the Pchlide binding by the conformational change of Asp84. Furthermore, in the L-protein–NB-protein complex from *P. marinus* [15], the two conserved residues, ChlN-Asp75 and ChlN-His77, corresponding to Asp84 and His86, are located at the docking region and are involved in the specific interaction with the L-protein (Fig. 5C). The binding of NA in this site would interfere with the docking of L-protein. Since the NB-protein is a symmetric complex of a catalytic unit BchN-BchB, a stoichiometry of NA, Pchlide, and NB-protein might be 2:2:1 in a hypothetical NA/Pchlide-bound NB-protein. Given that the inhibitor constant of NA (37 μM) are comparable with that of Pchlide (12 μM), it is worthwhile to try to prepare the NA/Pchlide-bound NB-protein for crystallographic analysis to identify the NA binding site.

In some diazotrophic prokaryotic groups including proteobacteria like *Rhodospirillum rubrum, Rhodobacter capsulatus,* and *Azospirillum brasilense*, the nitrogenase activity is post-translationally regulated by ADP-ribosylation [27,28]. Under nitrogen-sufficient conditions, the conserved Arg residue (Arg101 in *R. rubrum*) of Fe protein is modified by ADP-ribosylation. This modification sterically hinders the complex formation with MoFe protein resulting in blocking the electron transfer from Fe protein to MoFe-protein. In this ribosylation, the responsible enzyme DraT (dinitrogenase reductase ADP-ribosyltransferase) transfers the ADP-ribose moiety of NAD^+ into the Arg residue of Fe-protein and releases NA equimolar to ADP-ribose. A nitrogen-sufficient or light-limited condition induces the DraT-catalyzed ADP-ribosylation of Fe-protein, which is inevitably accompanied by the release of NA, in *R. capsulatus*. The intracellular NA concentration was estimated to be 90 μM at the maximum based on the concentration of Fe protein and the ratio of ADP-ribosylated form [29] with our empirical estimation of the cellular protein concentration of 500 mg $ml_{cell\ volume}^{-1}$. In the *in vitro* analysis, DPOR showed only about 30% activity in the presence of 100 μM NA. Therefore, the released NA might significantly reduce DPOR activity in *R. capsulatus* under conditions where most of the Fe protein is modified by ADP-ribosylation. This elaborate ADP ribosylation mechanism switches off the activity of nitrogenase and would reduce the activity of DPOR simultaneously in response to some environmental changes such as a sudden decrease of the energy level by dark. Further *in vivo* and *in vitro* analyses with *R. capsulatus* cells are needed to confirm the probable physiological significance of NA inhibition of DPOR.

Further biochemical analysis using the newly identified inhibitor NA will help elucidate the reaction mechanism, especially the intra-molecular electron transfer from the NB-cluster to Pchlide, which is coupled with the proton transfer to Pchlide, on the firm structural basis.

Acknowledgements

We thank Tadashi Mizoguchi and Hitoshi Tamiaki for providing Chl *c*. We thank Carl E. Bauer and Toshiharu Hase for the initial analysis of DPOR with crude extracts of *R. capsulatus*. We also thank Tatsuo Omata and Kazuki Terauchi for valuable discussion. This work was supported by Grants-in-Aid for Scientific Research Nos. 19570036, 20200063, 23370020 (to Y.F.) and for Challenging Exploratory Research No. 23655166 (to S.I.) from Japan Society for the Promotion of Science (JSPS), the Advanced Low Carbon

Technology Research and Development Program (ALCA), and by Precursory Research for Embryonic Science and Technology (PRESTO) of the Japan Science and Technology Agency (JST). J.N. and T.K. are also grateful for a Fellowship from the JSPS for Japanese Junior Scientists (19010733) and (24008402), respectively.

References

[1] Chew, A.G. and Bryant, D.A. (2007) Chlorophyll biosynthesis in bacteria: the origins of structural and functional diversity. Annu. Rev. Microbiol. 61, 113–129.
[2] Masuda, T. and Fujita, Y. (2008) Regulation and evolution of chlorophyll metabolism. Photochem. Photobiol. Sci. 7, 1131–1149.
[3] Fujita, Y. and Bauer, C.E. (2003) The light-independent protochlorophyllide reductase: a nitrogenase-like enzyme catalyzing a key reaction for greening in the dark in: Chlorophylls and Bilins: Biosynthesis, Synthesis, and Degradation (Kadish, K., Smith, K.M. and Guilard, R., Eds.), pp. 109–156, Academic Press, Amsterdom.
[4] Moser, J. and Bröcker, M.J. (2011) Enzymatic systems with homology to nitrogense in: Nitrogen Fixation, Methods and Protocols (Ribbe, M.W., Ed.), pp. 67–77, Springer Science+Business Media.
[5] Muraki, N., Nomata, J., Ebata, K., Mizoguchi, T., Shiba, T., Tamiaki, H., Kurisu, G. and Fujita, Y. (2010) X-ray crystal structure of the light-independent protochlorophyllide reductase. Nature 465, 110–114.
[6] Bröcker, M.J., Schomburg, S., Heinz, D.W., Jahn, D., Schubert, W.D. and Moser, J. (2010) Crystal structure of the nitrogenase-like dark operative protochlorophyllide oxidoreductase catalytic complex $(ChlN/ChlB)_2$. J. Biol. Chem. 285, 27336–27345.
[7] Masuda, T. and Takamiya, K. (2004) Novel insights into the enzymology, regulation and physiological functions of light-dependent protochlorophyllide oxidoreductase in Angiosperms. Photosynth. Res. 81, 1–29.
[8] Sytina, O., Heyes, D., Hunter, C., Alexandre, M., van Stokkum, I., van Grondelle, R. and Groot, M. (2008) Conformational changes in an ultrafast light-driven enzyme determine catalytic activity. Nature 456, 1001–1004.
[9] Reibothe, C., El Bakkouri, M., Buhr, F., Muraki, N., Nomata, J., Kurisu, G., Fujita, Y. and Reinbothe, S. (2010) Chlorophyll biosynthesis: spotlight on protochlorophyllide reduction. Trends Plant Sci. 15, 614–622.
[10] Nomata, J., Mizoguchi, T., Tamiaki, H. and Fujita, Y. (2006) A second nitrogenase-like enzyme for bacteriochlorophyll biosynthesis – Reconstitution of chlorophyllide *a* reductase with purified X-protein (BchX) and YZ-protein (BchY-BchZ) from *Rhodobacter capsulatus*. J. Biol. Chem. 281, 15021–15028.
[11] Tsukatani, Y. et al. (2013) An unexpectedly branched biosynthetic pathway for bacteriochlorophyll *b* capable of absorbing near-infrared light. Sci. Rep. 3, 1217.
[12] Fujita, Y. and Bauer, C. (2000) Reconstitution of light-independent protochlorophyllide reductase from purified BchL and BchN-BchB subunits. *In vitro* confirmation of nitrogenase-like features of a bacteriochlorophyll biosynthesis enzyme. J. Biol. Chem. 275, 23583–23588.
[13] Nomata, J., Swem, L., Bauer, C. and Fujita, Y. (2005) Overexpression and characterization of dark-operative protochlorophyllide reductase from *Rhodobacter capsulatus*. Biochim. Biophys. Acta 1708, 229–237.
[14] Sarma, R., Barney, B., Hamilton, T., Jones, A., Seefeldt, L. and Peters, J. (2008) Crystal structure of the L protein of *Rhodobacter sphaeroides* light-independent protochlorophyllide reductase with MgADP bound: a homologue of the nitrogenase Fe protein. Biochemistry 47, 13004–13015.
[15] Moser, J., Lange, C., Krausze, J., Rebelein, J., Schubert, W.D., Ribbe, M.W., Heinz, D.W. and Jahn, D. (2013) Structure of ADP–aluminium fluoride-stabilized protochlorophyllide oxidoreductase complex. Proc. Natl. Acad. Sci. USA 110, 2094–2098.
[16] Shioi, Y., Doi, M. and Böddi, B. (1988) Selective inhibition of chlorophyll biosynthesis by nicotinamide. Arch. Biochem. Biophys. 267, 69–74.
[17] Wong, K.K. (1978) 4-Vinyl protochlorophyllide excretion by *Rhodopseudomonas gelatinosa* in nicotinamide-enriched medium. Plant Sci. Lett. 13, 269–273.
[18] Nomata, J., Kitashima, M., Inoue, K. and Fujita, Y. (2006) Nitrogenase Fe protein-like Fe–S cluster is conserved in L-protein (BchL) of dark-operative protochlorophyllide reductase from *Rhodobacter capsulatus*. FEBS Lett. 580, 6151–6154.
[19] Nomata, J., Ogawa, T., Kitashima, M., Inoue, K. and Fujita, Y. (2008) NB-protein (BchN-BchB) of dark-operative protochlorophyllide reductase is the catalytic component containing oxygen-tolerant Fe–S clusters. FEBS Lett. 582, 1346–1350.
[20] Yamamoto, H., Nomata, J. and Fujita, Y. (2008) Functional expression of nitrogenase-like protochlorophyllide reductase from *Rhodobacter capsulatus* in *Escherichia coli*. Photochem. Photobiol. Sci. 7, 1238–1242.
[21] Kondo, T., Nomata, J., Fujita, Y. and Itoh, S. (2011) EPR study of 1Asp-3Cys ligated 4Fe–4S iron–sulfur cluster in NB-protein (BchN-BchB) of a dark-operative protochlorophyllide reductase complex. FEBS Lett. 585, 214–218.
[22] Kaiser, J.T., Hu, Y., Wiig, J.A., Rees, D.C. and Ribbe, M.W. (2011) Structure of precursor-bound NifEN: a nitrogenase FeMo cofactor maturase/insertase. Science 331, 91–94.
[23] Duyvis, M.G., Wassink, H. and Haaker, H. (1996) Formation and characterization of a transition state complex of *Azotobacter vinelandii* nitrogenase. FEBS Lett. 380, 233–236.
[24] Renner, K.A. and Howard, J.B. (1996) Aluminum fluoride inhibition of nitrogenase: stabilization of a nucleotide. Fe–protein. MoFe–protein complex. Biochemistry 35, 5353–5358.
[25] Schindelin, H., Kisker, C., Schlessman, J.L., Howard, J.B. and Rees, D.C. (1997) Structure of $ADP{\cdot}AlF_4$–stabilized nitrogenase complex and its implications for signal transduction. Nature 387, 370–376.
[26] Takahashi, R., Nakamura, S., Nakazawa, T., Minoura, K., Yoshida, T., Nishi, Y., Kobayashi, Y. and Ohkubo, T. (2010) Structure and reaction mechanism of human nicotinamide phosphoribosyltransferase. J. Biochem. 147, 95–107.
[27] Huergo, L.F., Pedrosa, F.O., Muller-Santos, M., Chubatsu, L.S., Monteiro, R.A., Merrick, M. and Souza, E.M. (2012) P_{II} signal transduction proteins: pivotal players in post-translational control of nitrogenase activity. Microbiology 158, 176–190.
[28] Nordlund, S. and Högbom, M. (2013) ADP-ribosylation, a mechanism regulating nitrogenase activity. FEBS J. 280, 3484–3490.
[29] Yakunin, A.F., Laurinavichene, T.V., Tsygankov, A.A. and Hallenbeck, P.C. (1999) The presence of ADP-ribosylated Fe protein of nitrogenase in *Rhodobacter capsulatus* is correlated with cellular nitrogen status. J. Bacteriol. 181, 1994–2000.